TURBULENT BOUNDARY LAYER FLOW SIMULATIONS OVER URBAN-LIKE ROUGHNESS USING LES

Kojiro Nozawa
Institute of Technology,
Shimizu Corporation
3-4-17 Etchujima, Koto-ku, Tokyo 135-8530, Japan
nozawa@shimz.co.jp

Tetsuro Tamura
Department of Environmental Science and Technology,
Tokyo Institute of Technology
4259 Nagatsuta, Midori-ku, Yokohama 226-8502, Japan
tamura@depe.titech.ac.jp

ABSTRACT

In this study, large eddy simulations of boundary layer flows over large-scale roughness have been performed targeting the experiments conducted by Cheng and Castro (2002). In order to duplicate the experimental conditions, the quasi-periodic boundary method for rough-wall boundary flows was applied to the inlet boundary conditions. The spatial variation of vertical profiles of mean and fluctuation velocities are studied in detail and compared to the experimental data. We focus on the influence on the spatial variations of turbulence structure deduced by large-scale roughness. The characteristics of the turbulent boundary layer flows over urban-like roughness (with a roughness area density of 25% and a boundary layer height ratio δ/h around 7) were different from the common homogenous roughness with δ/h larger than 50. The variable height of the roughness elements increased the zero-plane displacement height and the roughness length compared to those of uniform height roughness.

INTRODUCTION

The turbulence characteristics of the boundary layer flows over urban terrains are different from those of well-studied homogenous rough-wall turbulent boundary layer flows. In homogenous rough-wall turbulent boundary layer flows the upper limit of the roughness sublayer is from $2-5h$ and the inertial sublayer, which correspond with the logarithmic layer, is approximately 15% of boundary layer thickness (Jiménez, 2004). While the most of the urban terrain have small δ/h, it could be less than 20 in the case of a huge city. The roughness sublayer may extend to a significant height and the inertial sublayer then becomes squeezed between the roughness sublayer and the outer layer (Cheng and Castro, 2002). Cheng and Castro measured the spatially averaged mean velocity of the turbulent boundary layer flows over an urban-type surface ($\delta/h = 7$) in a wind tunnel and identified the upper limit of the inertial sublayer to be $2.3-2.4h$, where h is the cube height. Besides, the turbulence characteristics of turbulent boundary layer flows over relative large-scale roughness have not been well studied compared to those of homogenous rough-wall turbulent boundary layer flows.

The randomness of roughness size and roughness distribution of urban terrain may influence the characteristics of the boundary layer flows. The mean height and the mean roughness density may not be only parameters for the urban-like roughness. Grimmond and Oke (1999) suggested that an array of elements with variable heights is rougher than one with uniform heights.

The objectives of this study are to simulate the flows over large-scale inhomogenous roughness using LES and compare the turbulence characteristics with those of Cheng and Castro's (2002). The turbulence characteristics of a boundary layer flow over random height roughness is compared to those of a boundary layer flow over uniform height roughness using flow by visualizing vortical structures using second invariant of velocity gradient tensor.

NUMERICAL METHODS

The Navier-Stokes equations for an incompressible fluid combined with subgrid-scale turbulent viscosity are used for the large-eddy simulation. The filtered equation of continuity and Navier-Stokes equations can be described as follows:

$$\frac{\partial \bar{u}_i}{\partial x_i} = 0 \quad (1)$$

$$\frac{\partial \bar{u}_i}{\partial t} + \frac{\partial \bar{u}_j \bar{u}_i}{\partial x_j} = -\frac{\partial \bar{p}}{\partial x_i} + \frac{\partial \tau_{ij}}{\partial x_j} + Re^{-1}\frac{\partial^2 u_i}{\partial x_k \partial x_k} \quad (2)$$

$$\tau_{ij} = -2\nu_{sgs}\bar{S}_{ij} \quad (3)$$

$$\nu_{sgs} = C\Delta^2|\bar{S}| \quad (4)$$

where Δ is the filter size, $\bar{S}_{ij}$ is the velocity gradient tensor and $|\bar{S}|$ is $\sqrt{2\bar{S}_{ij}\bar{S}_{ij}}$. The dynamic procedure based on the Smagorinsky model is used to identify the model coefficient C. The model coefficient is determined through a least-squares minimization procedure (Lilly, 1992). Fourth-order central differencing scheme is used as spatial discretization and second-order time accurate explicit Adams-Bashforth differencing scheme is used for the convective terms and a part of the SGS turbulent diffusion terms. The rest of the diffusion term is treated semi-implicitly by using Crank-Nicolson formulation. The Reynolds number based on the free stream velocity and the boundary layer thickness is 9.3×10^4.

Simulating Spatial Developing Boundary Layer Using LES

The quasi-periodic boundary condition is introduced in streamwise direction to simulate the spatially developing boundary layers. The quasi-periodic boundary condition was proposed by Lund (1998) and modified by Nozawa and Tamura (2001) to apply to a rough-wall turbulent boundary layer flow. In this method the velocities at the recycle station are rescaled and reintroduced at the inlet and the outflow boundary is set far downstream of the recycle station (Fig.1). The rescaling of the velocity is done by decomposing the velocities into mean and fluctuating parts and applying the appropriate scaling laws to each component separately. Velocity fluctuations in the inner and outer regions are rescaled according to the ratio of friction velocities at the inlet and at the recycle station. The mean velocities are rescaled according to the "law of the wall" in the inner region and a "velocity defect law" in the outer region.

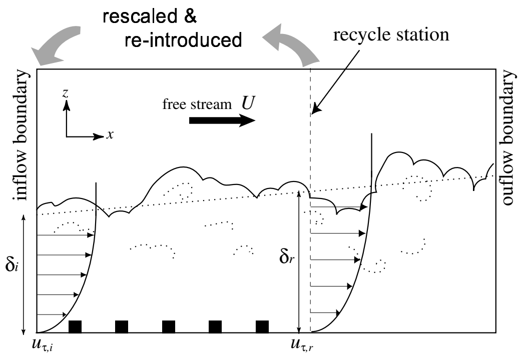

Figure 1: Schematic presentation of Lund's method with roughness blocks.

The method is originally limited to the generation of turbulent boundary layer over smooth surfaces that determine the rescaling parameter $\gamma(= u_{*,inst}/u_{*,recy}$, subscript "*inlt*"; quantity at inlet, subscript "*recy*": quantity at recycle station) in the form

$$\gamma = \beta^{-1/8} \tag{5}$$

, where β is the ratio of momentum thickness(θ) at inlet to momentum thickness at recycle station (Lund, 1998). We apply the resistance formula of sand-roughened plate by Prandtl (Schliching, 1979) to apply the quasi-periodic boundary condition to the flow over rough surface. In the modified method the friction velocity ratio γ can be deduced as follows (Nozawa and Tamura, 2001),

$$\beta^{-1} = 1 + \frac{c_f'(x)}{2\theta_{inlt}} \frac{\ell}{1-r} \left\{ \gamma^{2-2/r} - 1 \right\}. \tag{6}$$

In the equation ℓ is the estimated distance from the leading edge of the turbulent boundary layer , c_f' is the coefficient of skin friction of sand-roughened plate by Prandtl and r is

$$r = \frac{3.95}{2.87 + 1.58 \log \frac{\ell}{k_s}}, \tag{7}$$

where k_s is equivalent sand roughness. The periodic boundary conditions for velocities and pressure are applied in spanwise direction. At the outflow boundary the convective-type boundary condition is applied. The boundary conditions on the top surface of the computational domains are

$$\frac{\partial U}{\partial z} = 0, V = U_0 \frac{d\delta^*}{dx}, \frac{\partial W}{\partial z} = 0, \tag{8}$$

where U_0 is the free stream velocity and δ^* is the displacement thickness of the boundary layer.

Roughness Surfaces

The computational domains for the simulations are $88h \times 40h \times 20h$ in longitudinal(x), vertical(y) and lateral(z) directions respectively, where h is the height of the cubic roughness elements (Fig.2). The uniform cubic blocks are placed in staggered pattern following the experiments (Cheng and Castro, 2002). The roughness density defined as the ratio of frontal area to the floor area occupied by a single element is around 25%. The virtual boundary method proposed by Goldstein et al. (1994) and modified by Saiki and Bringen(1996) is carried out to set non-slip boundary condition on the surface of the roughness elements. In the case of random roughness, the height of the roughness elements is set as random variable, having five different heights chosen from a normal distribution with a mean and a standard deviation of $1.0h$ and $0.37h$ respectively. The tallest roughness element is $1.67h$ high and the lowest roughness element is $0.31h$ high.

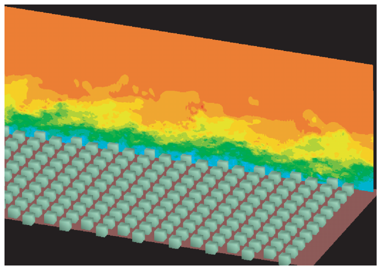

(a) uniform height roughness

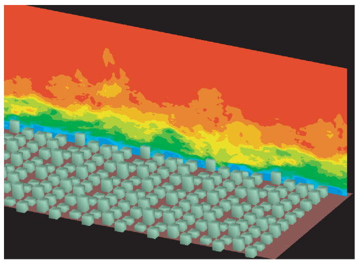

(b) random height roughness

Figure 2: Roughness surface and longitudinal velocity contour.

RESULTS

In this study the spatially averaged quantities are averaged over $8h$(x-direction)$\times 20h$(z-direction) plane. The nondimensional sampling time based on the freestream velocity and the boundary layer thickness is almost 90 in both uniform roughness and random roughness cases.

Flow Close to the Roughness

The vertical profiles of spatially averaged normal and shear stress are shown in Fig.3. The stresses are normalized by the friction velocities u_* which are deduced from the profiles of shear stress in both the roughness sublayer and the inertial sublayer. The shear stress profile of the random roughness has thicker constant stress layer compared to that of the uniform roughness. The profile of the random roughness slowly increases at $y < 1.3h$ and gradually decrease at

$y > 1.7h$, while that of uniform roughness has a peak at $y = 1.1h$ and gradually decrease at $y > 1.1h$. The both profiles almost collapse at $y > 2.2h$ although the stresses of the random roughness are larger than those of the uniform roughness at almost $y < 2.2h$. The vertical profiles of dispersive shear stresses are shown in Fig.4. The dispersive shear stress $\langle \bar{u}"\bar{v}" \rangle$ can be defined as follows.

$$\langle \bar{u}"\bar{v}" \rangle = \frac{1}{A} \int_s (\bar{u} - \langle \bar{u} \rangle)(\bar{v} - \langle \bar{v} \rangle) ds \qquad (9)$$

, where A is the spatially averaging area, angular brackets denotes spatially averaging and overbar denotes time averaging. The dispersive shear stress represents the contribution to momentum transfer from correlations between point-to-point variations in the time-averaged flow. The profiles have large values at $h < y < 2.2h$ and this range almost match with the height where the roughness blocks occupy the flow area in the horizontal plane. The departure of the vertical profiles between the random roughness and the uniform roughness at $y > h$ may cause the difference of the constant stress layer thickness. The range where random roughness has larger longitudinal and vertical stresses compared to those of the uniform roughness consist with the range the dispersive shear stress of the random roughness surpass that of the uniform roughness.

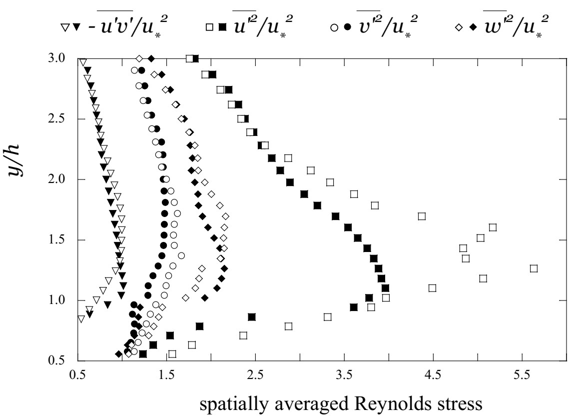

Figure 3: Spatially averaged stress normalized with friction velocity (u_*) and roughness height (h). black symbol, uniform roughness; white symbol, random roughness.

Figure 5 shows the instantaneous vortical structures of flows identified using isosurface of second invariant of velocity gradient tensor (Q). In this study Q is normalized by u_*^2. The white dashed line in the pictures indicate the height ($y = 2.2h$) where stress profiles of the uniform roughness and the random roughness begin to collapse. The small vortical structures almost fill the region ($y < 2.2h$) in the random roughness case while there are many void places in the uniform roughness case. These small vortical structures are strongly influenced by the local roughness elements directly. The positive values of second invariant of velocity gradient tensor (Q^+) are averaged over horizontal plane and its vertical profiles are shown in Fig.6 with their standard deviation profiles. These figures indicate that the random roughness case has vortical structures identified by large Q compared to those of the uniform roughness case at the range within random roughness heights.

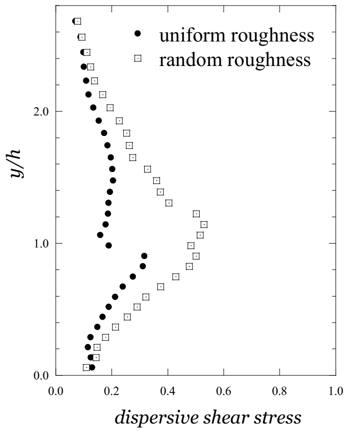

Figure 4: Dispersive shear stress normalized with friction velocity (u_*^2).

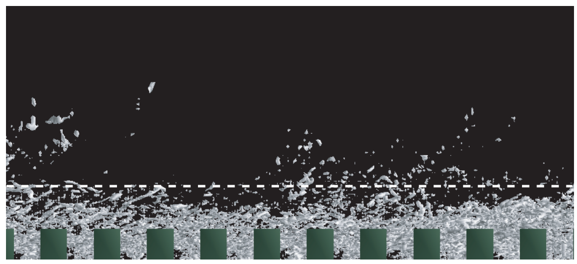

(a) uniform roughness

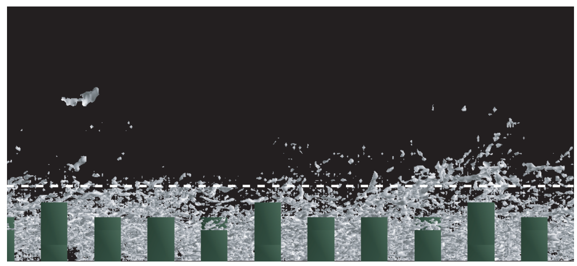

(b) random roughness

Figure 5: Instantaneous vortical structure identified using isosurface of second invariant of velocity gradient tensor ($Q = 100$).$- - -$,$y = 2.2h$.

Large Scale Structures in the Outer Region

In the upper region above the vortical structure in Fig.5 the large scale structures are dominant in the outer region (Fig.7). In this pictures the isosurface of second invariant of velocity gradient tensor normalized with its standard deviation (del Álamo et al., 2006), $Q/\sqrt{\overline{Q'(y)^2}}$, is applied to identify the outer region large scale structures which upraise their forward part in longitudinal direction. These large scale structures, whose length are approximately $1.7\delta \sim 3.5\delta$, are formed at almost even intervals horizontally. We couldn't see any evident difference between the uniform roughness and the random roughness in the size and the interval of the large scale structures in the outer region.

These large scale structures can also be distinguished

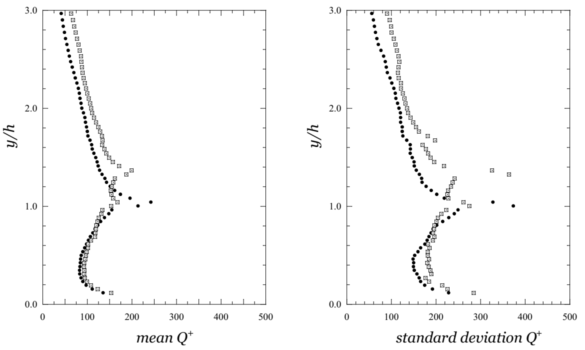

(a) mean   (b) standard deviation

Figure 6: Mean and standard deviation of the second invariant of velocity gradient tensor (Q^+). black symbol, uniform roughness; white symbol, random roughness.

from the picture of the instantaneous longitudinal velocity fluctuation contour on a horizontal plane at $y = 0.6\delta$. The boundary layer thickness δ is approximately $6h$ in this study. The large scale low speed region could be found in both uniform and random roughness cases. The axes of these structures are leaning to the lateral direction. The low speed region correspond to the region where the large scale structures identified using $Q/\sqrt{\overline{Q'(y)^2}}$. The length of the low speed regions indicated by dashed line circles in the pictures are 2.9δ (longitudinal) $\times$ 0.9δ(lateral) in the uniform roughness case and 3.0δ(longitudinal) $\times$ 1.5δ(lateral) in the random roughness case. Tsubokura and Tamura (2003) conducted the large eddy simulation of high Reynolds number (Re_τ=590, 1180) fully developed turbulent channel flows and found large-scale streaky patterns in the outer-layer, whose longitudinal and lateral size reach about three times and twice as large as the channel-half width respectively. The size of the low speed regions appeared in the turbulent boundary layer flows over urban-like roughness consist with the size of the streaky patterns found in the fully developed turbulent channel flows.

Spatially Averaged Vertical Mean and Stress Profiles

The mean velocities are normalized using the friction velocity which was deduced from the shear stress profiles (Fig.9). The roughness length y_0 and zero-plane displacement height d are identified fitting the mean velocity profiles to the log-law. The zero-plane displacement height and the roughness length of the random roughness is $1.14h$ and $0.04h$ respectively and both are 30% larger than those of the uniform roughness. These results are consistent with the experimental result (Cheng and Castro, 2002), that roughness length is dependent on the standard deviation of height variability in roughness elements. The zero-plane displacement height deduced by using the method (Jackson, 1981) which assumes that it is the mean height of momentum absorption by the surface (Raupach et al., 1991) was too small to fit the mean velocity profiles with the log-law.

The vertical profiles of spatially averaged stress are plotted against $(y - d)/\delta$ in Fig.10. The profiles of the random roughness and the uniform roughness collapse well at $(y - d)/\delta > 0.2$ in all stresses. The ratios σ_u/u_*,σ_v/u_* and σ_w/u_* take values of approximately 2.1, 1.4 and 1.1 respectively at 10% of the boundary layer thickness in the typical wind tunnel test, whose δ/h were 9-20 (Raupach et al., 1991). The profiles of both cases are in the range uncertainties in the wind tunnel test. These results indicate that the difference in turbulence characteristics of flows close to the roughness between the uniform roughness and the random roughness is limited to almost $2.2h$ even though the tallest roughness height in the random roughness is $1.67h$.

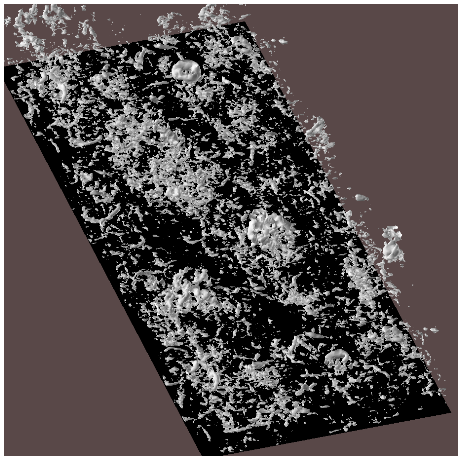

(a) uniform roughness

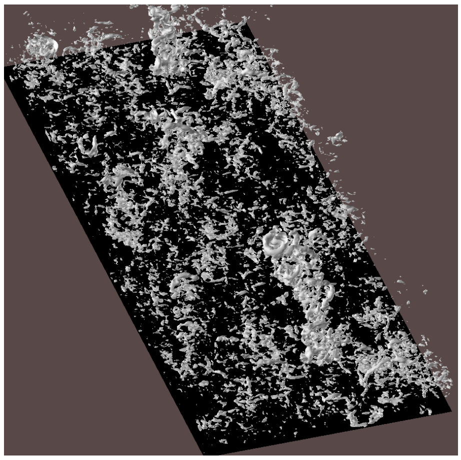

(b) random roughness

Figure 7: Instantaneous isosurface of the second invariant of velocity gradient tensor normalized with its standard deviation ($Q/\sqrt{\overline{Q'(y)^2}} = 1.0$).

SUMMARY

The large eddy simulation of spatially developing rough-wall turbulent boundary layer flows has been performed to study the effect of urban-like roughness on the turbulence structure. The random roughness case had large dispersive shear stress at $h < y < 2.2h$ and this may cause the thicker constant flux layer compared to that of the uniform roughness case. The random roughness case had vortical structures identified by large second invariant of velocity gradient tensor (Q) compared to those of the uniform roughness case. The zero-plane displacement height and the roughness length of the random roughness case was $1.14h$ and $0.04h$

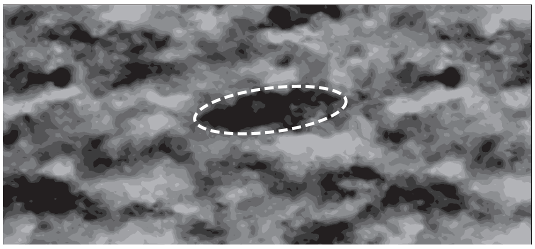

(a) uniform roughness

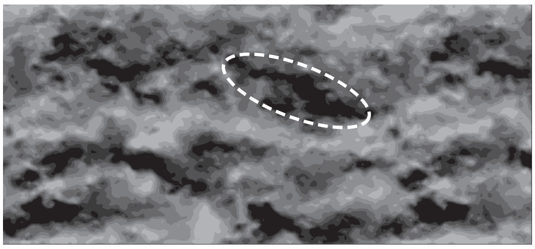

(b) random roughness

Figure 8: Instantaneous longitudinal velocity fluctuation ($\frac{u-\langle u\rangle}{\sigma_u}$) on an $x-z$ plane at $y = 0.6\delta$. white, high speed region; black low speed region.

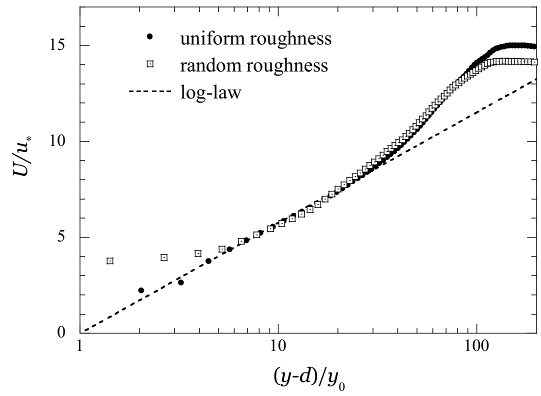

Figure 9: Spatially averaged mean velocity normalized with friction velocity (u_*).

respectively, and both were almost 30% larger than those of the uniform roughness case. The difference in turbulence characteristics of flows close to the roughness between the uniform and the random roughness was limited to almost $2.2h$ and the mean and stresses vertical profiles of the flows normalized with the friction velocity (u_*), zero-plane displacement height (d) and boundary layer thickness (δ) were in good agreement in the outer region.

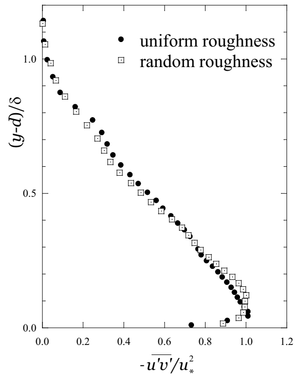

(a) shear stress

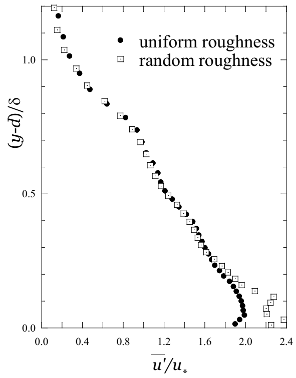

(b) longitudinal stress

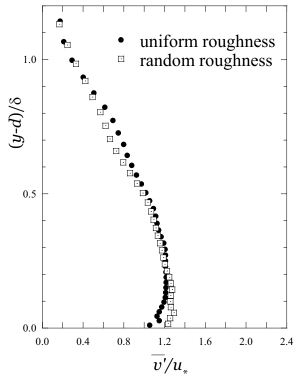

(c) vertical stress

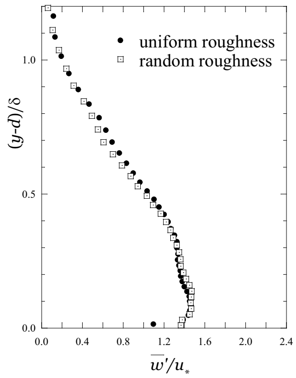

(d) lateral stress

Figure 10: Spatially averaged stresses normalized with friction velocity (u_*), zero-plane displacement height (d) and boundary layer thickness (δ).

REFERENCES

Cheng, H. and Castro, I. P., 2002, "Near Wall Flow Over Urban-Like Roughness", Boundary-Layer Meteorology, 104, pp. 229–259.

del Álamo, J. C., Jiménez, J., Zandonade, P. and Moser, R. D., 2006, "Self-similar vortex clusters in the turbulent logarithmic region", J. Fluid Mech., 561, pp.329–358.

Goldstein, D., Handler, R., and Sirovich, L., 1993, "Modeling a no-slip flow boundary with an external force field", J. Comp. Phys. 105, pp.354–366.

Grimmond, C. S. B. and Oke, T. R., 1999, "Aerodynamics Properties of Urban Areas Derived from Analysis of Surface Form", J. Appl. Meteorol., 38, pp.1262–1292.

Jackson, P. S., 1981, "On the displacement height in the logarithmic velocity profile", J. Fluid Mech., 111, pp.15–25.

Jiménez, J., 2004, "Turublent flows over rough walls", Annu. Rev. Fluid Mech. 36, pp.173–196.

Lilly, D. K., 1992, "A proposed modification of the Germano subgrid-scale closure method", Phys. Fluids A4, 3, pp. 633-635.

Lund, T. S., Wu, X. and Squires, K. D., 1998, "Generation of turbulent inflow data for spatially-developing boundary layer simulations",J. Comp. Phys., 140, pp. 233–258.

Nozawa, K. and Tamura, T., 2001, "Simulation of rough-wall turbulent boundary layer for LES inflow data", Proc. Turbulent Shear Flow Phenomena.

Raupach, M. R., 1981, "Conditional statics of Reynolds stress in rough-wall and smooth-wall turbulent boundary layers", J. Fluid Mech., 108, pp.363–382.

Raupach, M. R., Antonia, R. A. and Rajagopalan, S., 1991,"Rough-wall turbulent boundary layers", Appl. Mech. Rev., 44, pp.1–25.

Saiki, E. M. and Biringen, S., 1996, "Numerical simulation of a cylinder in uniform flow: application of a virtual boundary method", J. Comp. Phys., 123, pp.450–465.

Schlichting, H., 1979, "Boundary-Layer Theory, 7th Edition", McGraw-Hill Book Company.

Tsubokura, M. and Tamura, T., 2003, "On the large-scale flow motions in fully developed turbulent channel flow", Trancations of the Japan Society of Mech. Eng., B,69, 680, pp.81–88.